IMMUNOLOGY

Therapeutic blockade of activin-A improves NK cell function and antitumor immunity

Jai Rautela[1,2]*, Laura F. Dagley[3]*, Carolina C. de Oliveira[4], Iona S. Schuster[5,6,7], Soroor Hediyeh-Zadeh[8], Rebecca B. Delconte[1], Joseph Cursons[8], Robert Hennessy[1], Dana S. Hutchinson[9], Craig Harrison[10], Badia Kita[11], Eric Vivier[12], Andrew I. Webb[3], Mariapia A. Degli-Esposti[5,6,7], Melissa J. Davis[8,13], Nicholas D. Huntington[1,2]*, Fernando Souza-Fonseca-Guimaraes[1,14]*†

Natural killer (NK) cells are innate lymphocytes that play a major role in immunosurveillance against tumor initiation and metastatic spread. The signals and checkpoints that regulate NK cell fitness and function in the tumor microenvironment are not well defined. Transforming growth factor–β (TGF-β) is a suppressor of NK cells that inhibits interleukin-15 (IL-15)–dependent signaling events and increases the abundance of receptors that promote tissue residency. Here, we showed that NK cells express the type I activin receptor ALK4, which, upon binding to its ligand activin-A, phosphorylated SMAD2/3 to suppress IL-15–mediated NK cell metabolism. Activin-A impaired human and mouse NK cell proliferation and reduced the production of granzyme B to impair tumor killing. Similar to TGF-β, activin-A also induced SMAD2/3 phosphorylation and stimulated NK cells to increase their cell surface expression of several markers of ILC1 cells. Activin-A also induced these changes in TGF-β receptor–deficient NK cells, suggesting that activin-A and TGF-β stimulate independent pathways that drive SMAD2/3-mediated NK cell suppression. Last, inhibition of activin-A by follistatin substantially slowed orthotopic melanoma growth in mice. These data highlight the relevance of examining TGF-β–independent SMAD2/3 signaling mechanisms as a therapeutic axis to relieve NK cell suppression and promote antitumor immunity.

INTRODUCTION

Natural killer (NK) cells play a well-established role in protecting against tumor initiation and metastasis and are the focus of numerous clinical attempts to harness their unique antitumor functions (*1*, *2*). Several biological factors directly suppress or limit NK cell function through a range of mechanisms in the context of malignant disease. These include tumor-derived metabolites such as adenosine (*3*, *4*), enzymes such as indoleamine 2,3-dioxygenase-1 (IDO1 or IDO) (*5*), an increase in the abundance of cytokine-inducible Src homology 2 (SH2)–containing protein (CIS, encoded by *Cish*) (*6*), a reduction in the abundance of the antiapoptotic proteins Bcl2 and Mcl1 (*7*–*9*), modulation of the abundance of the activating receptor natural killer group 2D (NKG2D) (*10*), expression of inhibitory receptors for major histocompatibility complex class I (MHC-I) (*11*, *12*), and transforming growth factor–β (TGF-β) (*13*, *14*).

TGF-β is a secreted protein that has three different isoforms: TGF-β1, TGF-β2, and TGF-β3. These isoforms are expressed in different tissues, with TGF-β1 being the most abundant and potent modulator of the immune system (*15*). TGF-β1 is a pleiotropic cytokine produced by several cell subtypes [including tumor cells, regulatory T (T_{reg}) cells, stromal fibroblasts, and various myeloid cell subsets] and is an important suppressor of the antitumor functions of NK cells in experimental tumor models (*13*, *16*, *17*). TGF-β1 reduces NK cell priming and activation, including both cytotoxicity and cytokine production, by suppressing the mammalian target of rapamycin (mTOR) pathway (*13*, *18*). Consistent with this, a previous study demonstrated that anti–TGF-β–neutralizing antibodies increase NK cell effector functions in vitro and in vivo (*19*).

TGF-β receptor I (TGF-βRI) and TGF-βRII are transmembrane receptors associated with serine and threonine kinases that, upon ligand binding, mediate the phosphorylation of the SMAD family of transcription factors (*20*). Although TGF-β is the best-described inducer of this pathway, other factors [including activin-A, activin-B, myostatin (GFF8), GDF11, nodal, and bone morphogenetic proteins (BMPs), which play a critical role in bone and muscular development] can also stimulate the phosphorylation of SMAD3 and SMAD3 (collectively referred to as SMAD2/3) (*21*–*23*). Activin-A binds to a set of receptors (including ALK4, ALK7, ActRIIA, and ActRIIB) that are distinct from those used by the TGF-β isoforms (*22*). Activin-A and its receptor dimer comprising ALK4 and ACVR2A or ACVR2B play a critical role in muscular development (*23*) and can be produced in large amounts by dendritic cells (DCs) or after acute inflammation (*24*, *25*).

[1]Division of Molecular Immunology, The Walter and Eliza Hall Institute of Medical Research and Department of Medical Biology, Faculty of Medicine, Dentistry and Health Sciences, University of Melbourne, Parkville, Victoria 3052, Australia. [2]Department of Biochemistry and Molecular Biology, Biomedicine Discovery Institute, Monash University, Clayton, Victoria, Australia. [3]Systems Biology and Personalized Medicine Division, The Walter and Eliza Hall Institute of Medical Research and Department of Medical Biology, University of Melbourne, Parkville, Victoria 3052, Australia. [4]Laboratório de Células Inflamatórias e Neoplásicas, Departamento de Biologia Celular, SCB, Centro Politecnico, Universidade Federal do Paraná, Curitiba, CEP 81531-980, PR, Brazil. [5]Immunology and Virology Program, Centre for Ophthalmology and Visual Science, University of Western Australia, Crawley, Western Australia, Australia. [6]Centre for Experimental Immunology, Lions Eye Institute, Nedlands, Western Australia, Australia. [7]Infection and Immunity Program and Department of Microbiology, Biomedicine Discovery Institute, Monash University, Clayton, Victoria, Australia. [8]Bioinformatics Division, The Walter and Eliza Hall Institute of Medical Research and Department of Medical Biology and Faculty of Medicine, Dentistry and Health Sciences, University of Melbourne, Parkville, Victoria 3052, Australia. [9]Monash Institute of Pharmaceutical Sciences, Monash University, Parkville, Victoria 3052, Australia. [10]Monash Biomedicine Discovery Institute, Monash University, Clayton, Victoria 3800, Australia. [11]Paranta Biosciences Limited, Melbourne, Victoria 3004, Australia. [12]Centre d'Immunologie de Marseille-Luminy, Aix Marseille Université, Inserm, CNRS, 13288 Marseille, France. [13]Faculty of Medicine, Dentistry and Health Sciences, University of Melbourne, Melbourne, Victoria 3010, Australia. [14]University of Queensland Diamantina Institute, University of Queensland, Translational Research Institute, Brisbane, Queensland, Australia.
*These authors contributed equally to this work.
†Corresponding author. Email: f.guimaraes@uq.edu.au

Although TGF-β signaling is a critical step in the differentiation of naïve $CD4^+$ T cells into $CD4^+$ $Foxp3^+$ T_{reg} cells, activin-A can also induce Foxp3 expression and promote the generation of T_{reg} cells (*26*, *27*). In breast and ovarian cancer cells, activin-A signaling induces the epithelial-mesenchymal transition (EMT), a malignant cellular reprogramming that is characteristic of TGF-β signaling (*28*, *29*). In addition, activin-related genes are increased in expression during breast cancer cell EMT (*30*). High circulating amounts of activin-A are associated with tumor progression and poor prognosis in patients with lung cancer (*31*). In addition, activin signaling reprograms macrophages into protumorigenic subsets that promote skin carcinogenesis (*32*). The biological activity of activin-A is inhibited by an endogenous inhibitor known as follistatin (FST) and also at the cell surface by TGFBR3 (betaglycan) (*33*). Studies have shown a correlation between reduced FST abundance and lower survival rates among patients with breast cancer and cutaneous melanoma (*34*, *35*). Similarly, low expression of *Tgfbr3* is prognostic of poor survival in renal cell carcinoma (*36*). Previous work showed that DC-derived activin-A reduced the activation of peripheral blood human NK cells and their production of cytokines (*37*). Although previous studies have hinted at the involvement of alternative SMAD2 or SMAD3 pathways in regulating human NK cell function, the precise mechanism and influence on NK cell biology are still to be elucidated.

The broader effect of TGF-β signaling on group 1 innate lymphoid cells [consisting of conventional NK (cNK) cells and type 1 innate lymphoid cells (ILC1) (*38*)] was demonstrated in the salivary gland and has generated renewed interest in the precise effect of TGF-β on NK cell functions within the tumor microenvironment (*39*). We previously identified a unidirectional reprogramming of cNK cells into ILC1-like cells that was driven by TGF-β in the tumor microenvironment. Transgenic mouse models with ablated or constitutive TGF-β signaling specifically in $NKp46^+$ cells had reduced numbers of ILC1s and cNK cells, respectively. TGF-β signaling also drives cNK cells to acquire a transitional ILC1-like phenotype both in vitro and in vivo by reducing the abundance of the transcriptional factor Eomesodermin (or Eomes) and increasing the abundance of tissue residency–related markers, such as tumor necrosis factor–related apoptosis-inducing ligand (TRAIL) and the collagen-binding protein integrin α-1 (CD49a) in the tumor microenvironment (*14*). A population of $NKp46^+CD49a^+$ cells was still observed in the tumor microenvironment of $NKp46^{cre/+}$*Tgfbr2*$^{fl/fl}$ mice, which suggests that a minor TGF-β–independent pathway for ILC1-like differentiation may exist. Here, we showed that activin-A stimulates an alternative SMAD signaling pathway that suppressed NK cell metabolism and cytotoxicity, ultimately inducing an increase in the abundance of tissue residency markers on NK cells.

RESULTS

Functional activin-A receptor expression on NK cells

Receptors for activin-A are classified as type 1 [ACVR1B (also known as ALK4) and ACVR1C (also known as ALK7)] and type 2 (ACVR2A and ACVR2B) receptors (*40*). Human NK cells are reported to express mRNA for activin-A receptors (ALK4, ACVRIIA, and ACVRIIB) and potentially respond to activin-A (*37*). Using available RNA-sequencing data (*41*–*43*), we compared the amounts of mRNAs for activin receptors in the following murine NK cell subsets: progenitors (pre-pro NK cells and NKP cells), immature ($CD27^+CD11b^{neg}$) NK cells, mature ($CD27^{neg}CD11b^+$) NK cells, and liver tissue-resident or ILC1 ($TRAIL^+CD49b^{neg}$) cells. All cell subsets expressed ALK4 mRNA, which declined in abundance as the NK cells matured, paralleling the expression pattern of TGF-βRII (Fig. 1A) and consistent with our previous report (*13*). However, we failed to detect mRNAs corresponding to the receptors ACVR2A, ACVR2B, and ACVR1C in these NK cell subsets (fig. S1).

A challenge in the field of TGF-β research is the highly conserved homology of this cytokine between species (*44*). Because of the presence of bovine TGF-β in conventional media containing fetal calf serum (FCS) (fig. S2), in our in vitro assays, we used medium free from animal-derived components to compare the effects of recombinant TGF-β versus activin-A. Using recombinant activin-A (rActivin-A), we observed that purified mouse NK cells exhibited increased amounts of phosphorylated SMAD2/3 in a concentration-dependent manner but not to the same degree as that found in cells treated with recombinant TGF-β (rTGF-β1) (Fig. 1, B and C). Similarly, both rTGF-β1 and rActivin-A (particularly at the highest concentration tested) inhibited NK cell proliferation in response to interleukin-15 (IL-15) (Fig. 1, D and E). We found that neither ligand induced NK cell death (fig. S3) (*7*) but rather suppressed the rate at which the NK cells divided (Fig. 1, D and E). These results suggest that NK cells responded to activin-A, albeit with less extensive SMAD2/3 phosphorylation than that induced by TGF-β and with less of an effect on proliferation.

Inhibition of proliferation is a notable consequence of TGF-β signaling in NK cells and is directly linked to the inhibition of metabolism mediated by mTOR (*13*). To relate these changes to cellular metabolism, we measured the extracellular acidification rate (ECAR) and oxygen consumption rate (OCR) of wild-type (WT) and *TgfbR2*-deficient NK cells in response to rActivin-A or TGF-β (Fig. 1, F and G). Unexpectedly, *TgfbR2*-deficient NK cells displayed at least twofold higher basal glycolysis (ECAR) and oxidative phosphorylation (OCR) compared to WT cells, suggesting that they exhibited constitutively enhanced metabolism in vitro. Although rTGF-β1 was unable to inhibit ECAR and OCR in *TgfbR2*-deficient NK cells, it completely suppressed metabolism in WT NK cells (Fig. 1, F and G). We found that rActivin-A inhibited both of these parameters in both WT and *TgfbR2*-deficient NK cells and that this effect was maximal at the lower concentration of rActivin-A, suggesting that minimal SMAD2/3 phosphorylation was required to suppress metabolism (Fig. 1, B and C). Together, these results suggest that the ALK4 pathway inhibits cellular metabolism in murine NK cells.

Activin signaling drives an increase in tissue residency marker abundance on NK cells

Lymphocytic tissue residency is characterized by decreased proliferation and the expression of tissue residence markers, such as the collagen-binding receptor CD49a (also known as ITGA1 and VLA-1), which functions as a cellular anchor (*45*). Parabiosis experiments demonstrated that tissue-resident $Eomes^{neg}CD49a^+$ NK cells, also known as ILC1s, are unable to migrate between parabiotic mice, whereas conventional $Eomes^+CD49a^{neg}$ NK cells (cNK) migrate freely (*46*). We previously showed that rTGF-β1 simultaneously increases CD49a cell surface abundance and reduces Eomes abundance in cNK cells in vitro. In addition, although TGF-βR2–deficient $NKp46^+$ cells are completely unresponsive to rTGF-β1 in vitro, CD49a is still detectable on a subset of these cells in vivo (*14*).

To investigate whether cNK to ILC1-like differentiation (characterized by reduced Eomes and increased CD49a abundance) could be

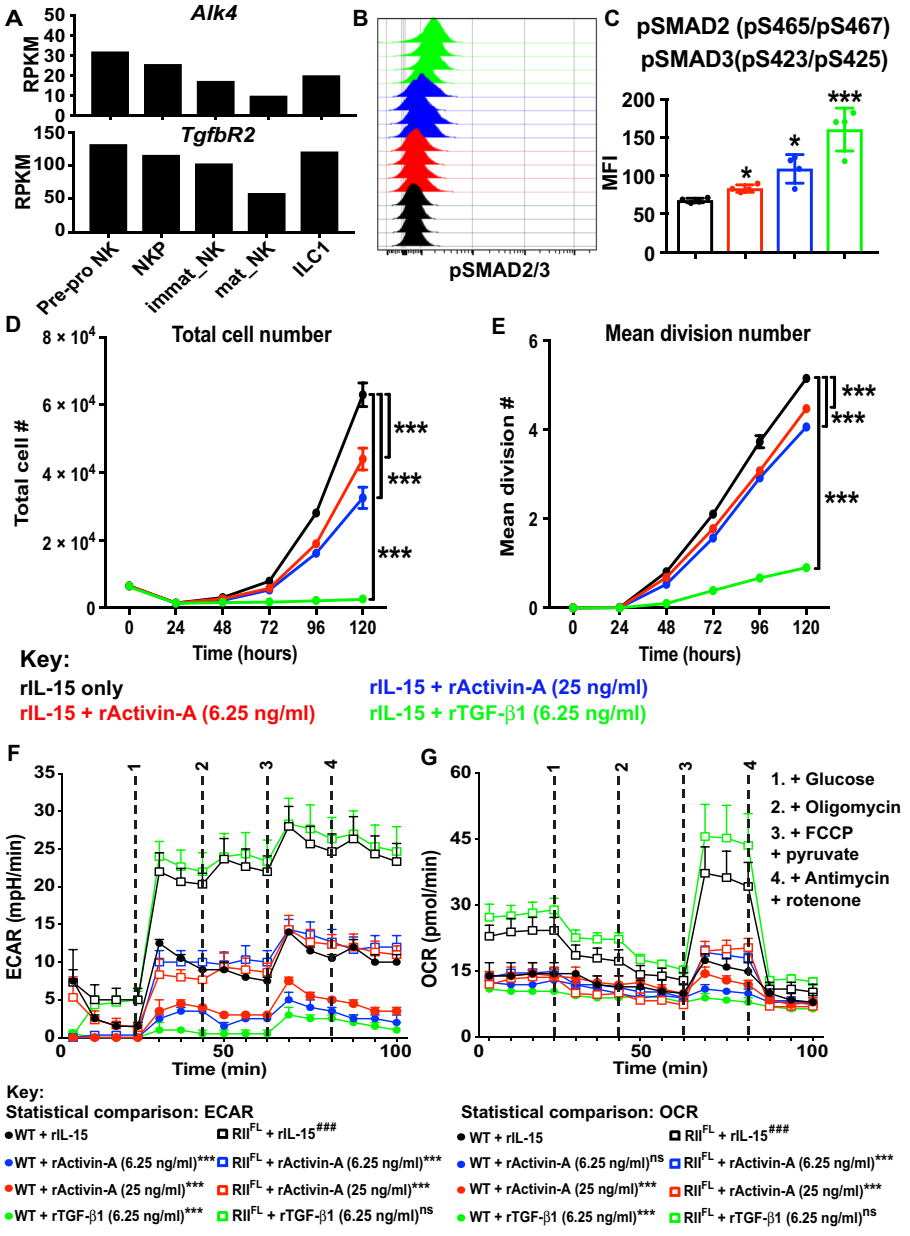

Fig. 1. Activin receptor expression and responsiveness in NK cells. (**A**) Analysis of the mRNA abundance of *Alk4* and TGF-βRII (*TgfbR2*) in pre-pro NK cells, NK cell progenitors (NKP), immature NK cells (immat_NK), mature NK cells (mat_NK), and liver ILC1s. Data are representative of two biological replicates. RPKM, reads per kilobase per million mapped reads. (**B** and **C**) Purified NK cells were cultured in the indicated concentrations of rActivin-A or rTGF-β1 for 1 hour, stained for pSMAD2/3, and analyzed by flow cytometry. Data represent biological replicates and are presented as histograms (B) or mean fluorescence intensity (MFI) of the pSMAD2/3 staining intensity (C). Data are means ± SEM of four biological replicates. Unpaired *t* tests were used for comparative statistical analysis. $^{*}P < 0.05$ and $^{***}P < 0.001$. (**D** and **E**) CellTrace Violet (CTV)–labeled NK cells were cultured in the presence of rIL-15 alone or in addition to the indicated concentrations of rTGF-β1 or rActivin-A. Total live cells in each division were enumerated at 24-hour intervals to determine their proliferation rate (mean division number). Results are from one representative biological replicate of three independent experiments. Data are means ± SEM of technical triplicates. Two-way ANOVA was used for statistical analysis. $^{***}P < 0.001$. (**F** and **G**) IL-15–expanded NK cells were cultured overnight (20 hours) in the presence of rIL-15 with or without the indicated concentrations of rActivin-A or rTGF-β1. Cells were then plated in glucose-free medium containing rIL-15 (5 ng/ml) for 3 hours, followed by transfer to gelatin-coated seahorse assay plates for measurement of extracellular acidification rate [ECAR; (F)] and oxygen consumption rate [OCR; (G)] every 7 min using a Seahorse XF^{e}96 analyzer. Data are means ± SEM of three biological replicates. The paired *t* test was used for statistical analysis. $^{***}P < 0.001$ for comparisons between the indicated stimulation within the WT or RII^{FL} groups; $^{\#\#\#}P < 0.001$ for comparisons between the WT and RII^{FL} cells. ns, not significant.

induced by rActivin-A similarly to rTGF-β1, we cultured highly purified (99 to 100% purity) splenic cNK cells (viable, CD3/CD19/F4-80/Ly6G/TCRβ^{neg}, CD49a^{neg}, NKp46^{+}, NK1.1^{+}, CD49b^{+}) from NKp46$^{cre/+}$ *TgfbR2*$^{fl/fl}$ mice and their corresponding littermate controls (NKp46$^{+/+}$*TgfbR2*$^{fl/fl}$) in animal component–free medium supplemented with rActivin-A or rTGF-β1. We then performed a global, label-free proteomics analysis of these NK cells to compare the protein expression profiles in the presence of rTGF-β1 or rActivin-A (Fig. 2, A to D). We identified similar patterns of protein expression between WT NK cells stimulated with either rTGF-β1 or rActivin-A and RII^{FL} cells stimulated with rActivin-A, but not rTGF-β1. Unexpectedly, rActivin-A was as efficacious as rTGF-β1 at increasing the surface abundance of CD49a on WT NK cells and, unlike TGF-β, also acted upon TGF-βR2–deficient NK cells (Fig. 2, A and D to F). We also identified a number of proteins that were consistently reduced in abundance in WT NK cells stimulated with either rTGF-β1 or rActivin-A and in RII^{FL} cells that were stimulated with rActivin-A but not rTGF-β1 (Fig. 2, A to D), including the proliferation marker Ki67, stathmin (STMN1), and the DNA binding protein IKZF1 (or Ikaros), an important transcriptional factor that maintains NK cell maturation and function (*47*).

We next addressed whether signaling induced by the simultaneous combination of activin-A and TGF-β could maximize the signaling effects of the SMAD2/3 pathway in NK cells using the measurement of CD49a and Ikzf1 abundance as a readout. We performed in vitro combinatorial experiments with both stimuli in different concentrations to measure synergistic effects on CD49a and Ikzf1 expression. The abundance of CD49a was increased by different concentrations of activin-A in WT and TGF-βRII–deficient NK cells and by TGF-β1 in WT cells (fig. S4A), consistent with our earlier data (Fig. 2, E and F); however, the addition of rTGF-β1 at different concentrations was unable to synergistically increase CD49a abundance in activin-A–treated WT cells (fig. S4B). Corroborating our global proteomics data, we also observed by intracellular fluorescence-activated cell sorting (FACS)

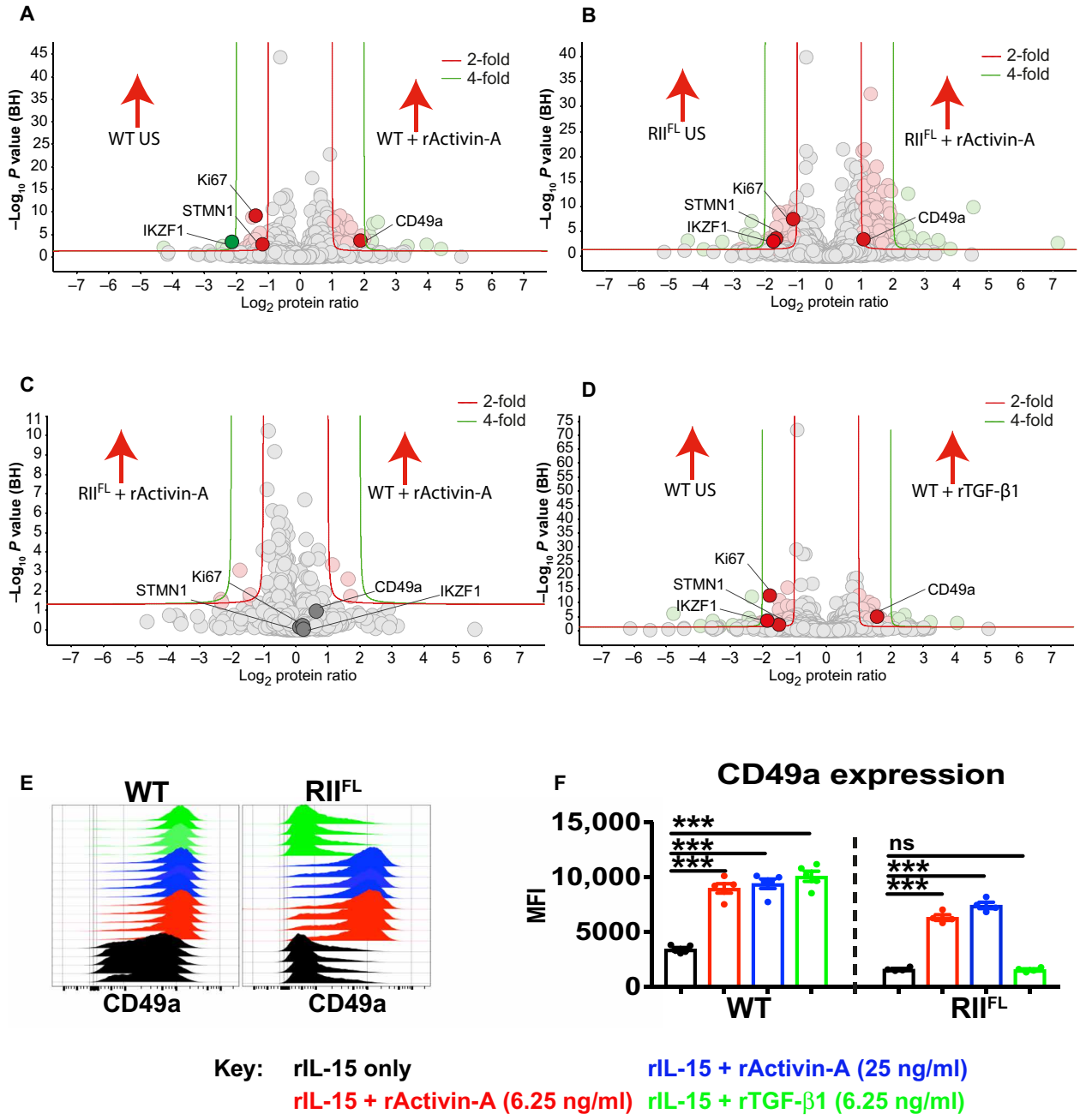

Fig. 2. Activin-A induces cellular differentiation cNK cells. (**A** to **D**) IL-15–expanded NK cells isolated from WT and RII^{FL} mice were cultured for 24 hours in the presence of rIL-15 with or without the indicated concentrations of rTGF-β1 or rActivin-A and then processed for label-free global proteomics analysis. Volcano plots illustrating the $\log_2$ protein ratios after quantitative pipeline analysis that compared rActivin-A stimulation versus unstimulated (US) NK cells in WT (A) and RII^{FL} (B) samples, rActivin-A stimulation between WT and RII^{FL} samples (C), or rTGF-β1 stimulation versus unstimulated NK cells in WT samples (D). Proteins were deemed to be differentially regulated if the $\log_2$ fold change in protein abundance was greater than twofold (red) or fourfold (green) and a −log10 *P* value of ≥1.3, equivalent to $P \leq 0.05$. (**E** and **F**) Purified splenic cNK cells from the spleens of RII^{FL} mice (NKp46$^{cre/+}$*Tgfbr2*$^{fl/fl}$) or their respective littermate control mice were cultured in medium containing rIL-15 (50 ng/ml) with or without the indicated concentrations of rActivin-A or rTGF-β1 for 48 hours. Cell surface CD49a expression (E and F) was determined by flow cytometry analysis, with data represented as histograms (E) or as MFI (F) for the indicated stimulation condition. Error bars represent the SEM, and each data point/histogram represents one independent biological replicate. Unpaired *t* tests were used for comparative statistical analysis. ***$P < 0.001$.

analysis (fig. S4, C and D) that the abundance of Ikzf1 was decreased by either activin-A or TGF-β1 in WT NK cells or by activin-A in TGF-βRII–deficient NK cells. In addition, and similarly to CD49a, Ikzf1 abundance was not further decreased in WT cells when rActivin-A and rTGF-β1 were combined. These findings suggest that activin signaling induces changes in NK cell phenotype that are reminiscent of those involved in NK cell cellular reprogramming mediated by TGF-β.

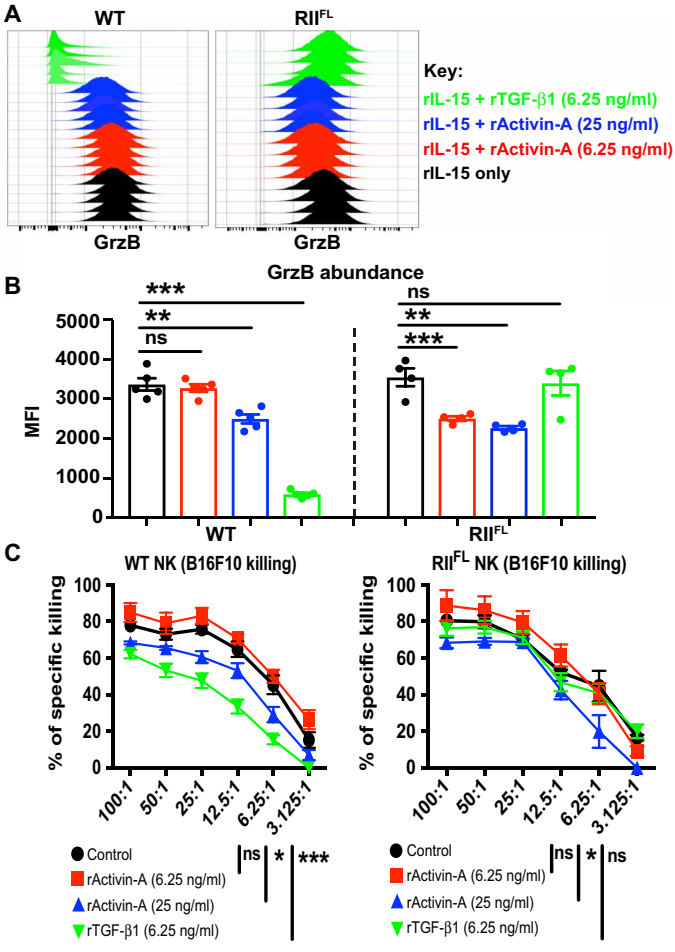

Fig. 3. Effects of activin signaling on NK cell–mediated cytotoxicity. (**A** and **B**) NK cells sorted from the spleens of five WT and four RII^{FL} mice were cultured in vitro for 5 days in medium containing rIL-15 (50 ng/ml) with or without the indicated concentrations of rActivin-A or TGF-β1. The cells were then fixed, permeabilized, and stained for intracellular GrzB and analyzed by flow cytometry. Data are shown as overlays (A) or as MFI (B), with each data point/histogram representing one independent biological replicate. Error bars represent SEM. One-way ANOVA was used for comparative statistical analysis. *$P < 0.05$ and **$P < 0.01$. (**C**) Sorted NK cells were cultured overnight (16 hours) in the presence of rIL-15 (50 ng/ml) with or without the indicated concentrations of rActivin-A or TGF-β1 in animal component–free medium and then tested against B16F10 target cells at various effector:target ratios in a 4-hour calcein-release cytotoxicity assay. Results are means ± SEM of two independent experiments. Two-way ANOVA was used for comparative statistical analysis. *$P < 0.05$ and ***$P < 0.001$.

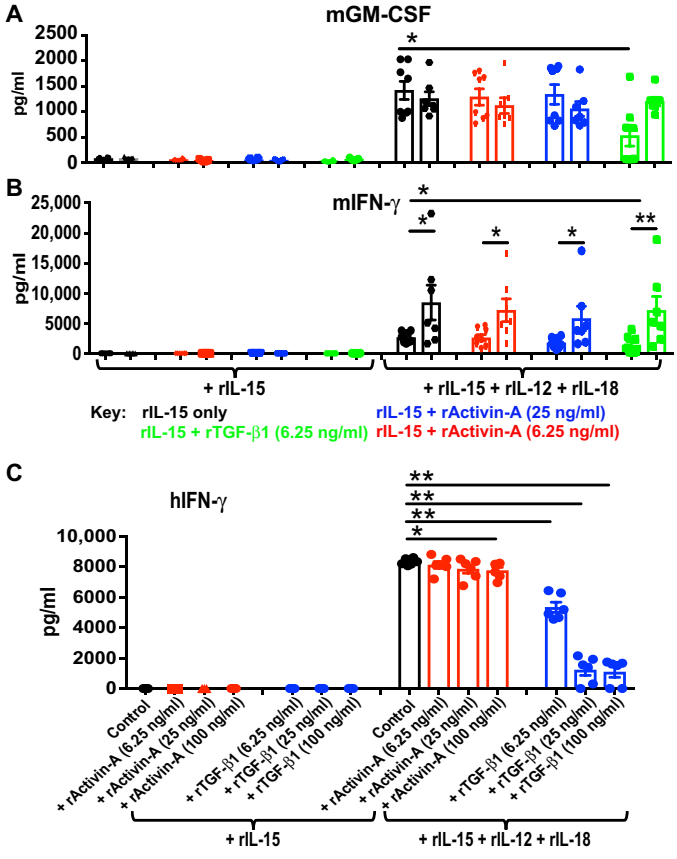

Fig. 4. Differential cytokine induction or suppression by activin-A and TGF-β signaling in NK cells. (**A** and **B**) NK cells sorted from the spleens of WT mice (data displayed in the first column of each group) or RII^{FL} mice (data displayed in the second column of each group) were cultured in medium containing rIL-15 (50 ng/ml) with or without rIL-12 (20 pg/ml) and rIL-18 (50 ng/ml) in the presence or absence of the indicated concentrations of rActivin-A or rTGF-β1 for 48 hours. The cell culture medium was then analyzed for the presence of secreted murine GM-CSF (A) and IFN-γ (B). (**C**) Human cord blood NK cells were isolated by negative selection and cultured in medium containing rIL-15 (50 ng/ml) with or without rIL-12 (20 pg/ml) and rIL-18 (50 ng/ml) in the presence or absence of the indicated concentrations of rActivin-A or rTGF-β1 for 48 hours. Results are expressed as means ± SEM of the concentration of IFN-γ in the culture medium. Each data point represents one independent biological replicate. The unpaired *t* test was used for comparative statistical analysis. *$P < 0.05$ and **$P < 0.01$.

Activin-A modulates NK cell–mediated killing

A previous study showed that rTGF-β1 inhibits NK cell cytotoxicity in vitro (*13*). Similarly, the constitutive activation of TGF-βR1 in NKp46^{+} cells completely abolishes the in vivo killing potential of NK cells (*14*). In addition to being a critical survival factor (*8*, *9*), IL-15 induces the production of granzyme B (GrzB) in NK cells (*48*). To test whether activin signaling also limited NK cell cytotoxicity, we cultured WT and TGF-βRII–deficient NK cells with IL-15 and exposed them to either TGF-β or activin. As expected, rTGF-β1 reduced the amount of GrzB in WT NK cells, whereas rActivin-A modestly reduced its abundance in both WT and TGF-βRII–deficient NK cells (Fig. 3, A and B). Consistent with this observation, we found that rTGF-β1 suppressed the NK cell–mediated killing of B16F10 melanoma cells to a greater extent than did rActivin-A (Fig. 3C). These results show a subtle but previously uncharacterized role for activin in suppressing NK cell cytotoxicity independently of canonical TGF-β signaling.

Distinct effects of activin and TGF-β signaling on cytokine secretion by NK cells

To further assess whether the activin and TGF-β signaling pathways had divergent effects on NK cell function, we assessed the cytokines secreted by purified WT or *Tgfbr2*$^{fl/fl}$ NK cells after stimulation for 48 hours with rIL-15 in the presence or absence of rActivin-A, rTGF-β1, rIL-12, or rIL-18. We found that TGF-β impaired the secretion of granulocyte-macrophage colony-stimulating factor (GM-CSF) in response to IL-12 and IL-18, whereas activin-A had no such effect (Fig. 4A). Interferon-γ (IFN-γ) production by NK cells is markedly increased in response to IL-12 or IL-18, which was not affected by

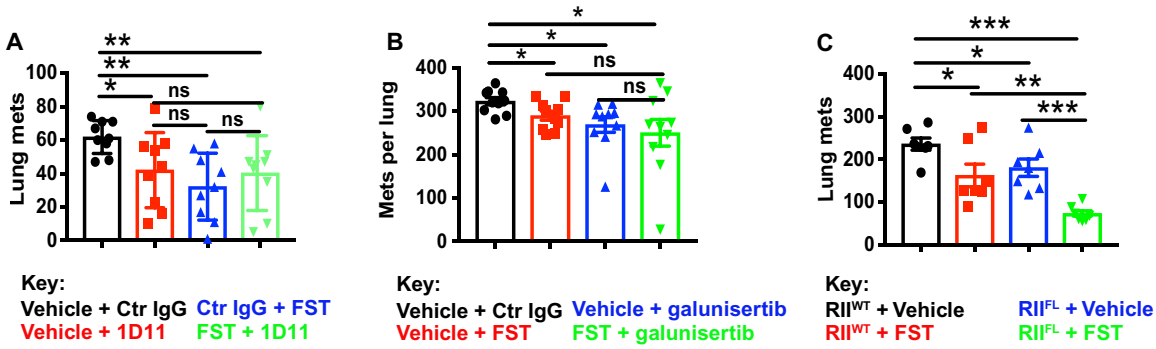

Fig. 5. Inhibition of activin-A or TGF-β signaling in vivo results in therapeutic benefit. (**A**) Groups of nine WT mice were injected intravenously with 2×10^5 B16F10 melanoma cells and treated with follistatin (FST) or vehicle (10 μg per mouse per day, intraperitoneal) starting 1 day after tumor inoculation. Neutralizing anti–TGF-β1/2/3 antibody (1D11) or control (Ctr) immunoglobulin G (IgG) was administered intraperitoneally at doses of 500 μg per mouse every 2 days, starting 1 day after tumor inoculation until the endpoint (14 days after tumor inoculation). (**B**) Groups of 10 WT mice were injected intravenously with 4×10^5 B16F10 melanoma cells and treated with FST as described for (A). Galunisertib was administered intraperitoneally at doses of 10 mg/kg per mouse at days 1, 3, 5, and 7 after tumor inoculation. (**C**) Groups of six or seven RII^{FL} mice (RII^{FL}) or their respective littermate controls mice (RII^{WT}) were injected intravenously with 4×10^5 B16F10 cells, with FST treatments and experimental endpoints as described for (A). (A to C) Symbols in the scatterplots represent the number of tumor nodules in the lung from individual mice (with means and SEM shown by error bars). The unpaired *t* test was used to compare differences between groups of mice as indicated. *$P < 0.05$, **$P < 0.01$, and ***$P < 0.01$.

either activin-A or TGF-β. Despite being phenotypically similar to WT NK cells, TGF-βRII–deficient NK cells produced notably more IFN-γ than did WT cells, suggesting that they were more activated in the absence of TGF-β signaling in vivo (Fig. 4B; similar to the higher basal metabolism indicated by higher OCR observed in Fig. 1G). To test whether these findings could be corroborated with human NK cells, human cord blood–derived NK cells were cultured for 48 hours in the same concentrations of IL-12, IL-15, and IL-18 that were used to treat mouse NK cells and in a range of activin-A or TGF-β concentrations. All of the TGF-β1 concentrations tested resulted in suppression of IFN-γ secretion in response to IL-12 or IL-18 stimulation, whereas only the highest concentration of activin-A used had the same effect (Fig. 4C). This result not only supports a previous report (*37*) that demonstrated similar effects in human peripheral blood–derived NK cells but also reveals that not all aspects of activin-A or TGF-β signaling are conserved between mouse and human cells.

Targeted inhibition of activin signaling in NK cell–dependent in vivo models of melanoma

Using clinical-grade FST (98% homologous between mouse and human), which is specific to activin-A and not to other BMP family members (fig. S5), we first tested whether it was possible to therapeutically enhance the highly NK cell–dependent immune response against the B16F10 melanoma model (*8*, *49*). FST was administered to tumor-bearing mice according to the manufacturer's recommendations and was compared to a TGF-β1/2/3–neutralizing antibody (clone 1D11.16.8) and the TGF-βRI kinase inhibitor galunisertib (also known as LY2157299), which has been validated for in vivo use (*50*–*52*). These experiments revealed that, similar to TGF-β blockade, FST statistically significantly reduced the number of lung metastases; however, no additive benefit was observed when both agents were combined (Fig. 5, A and B). In a different approach, we compared the effect of FST in the high B16F10 burden model using RII^{FL} mice or WT littermate controls and found that only FST statistically significantly reduced lung metastases (Fig. 5C); a more enhanced effect was observed when TGF-βRII was conditionally deleted in the NK cells (RII^{FL} mice) (Fig. 5C). These results suggest that in vivo inhibition of activin-A could improve tumor rejection by enhancing the innate effector functions of NK cells.

TGF-β signaling in NK cells induces the increased abundance of ILC1-like markers in vivo (*14*, *39*). Although the conditional deletion of the gene encoding TGF-βRII in $NKp46^+$ cells suggested that this increased abundance of ILC1-like markers could be largely prevented in vivo, alternative stimuli of the SMAD2/3 pathway likely compensated for the lack of TGF-β signaling. Murine cytomegalovirus (MCMV) infection was previously described to induce the increased abundance of ILC1-like molecules (e.g., TRAIL, CD49a, and CD69) (*53*) on salivary gland NK cells in a TGF-β–like manner (*39*). To assess whether these MCMV-induced changes in ILC1-like markers (e.g. CD49a, CD69, or TRAIL) could be therapeutically prevented, we treated MCMV-infected mice with FST, a TGF-β–neutralizing antibody, or a combination of both. None of the treatments prevented the increased expression of CD49a, CD69, or TRAIL on $NKp46^+$ cells in either the liver or salivary glands of the mice on day 6 after infection (fig. S6). We also did not observe any statistically significant differences in viral loads in the spleen, liver, or lungs of mice from the different treatment groups 6 days after infection (fig. S7). These data suggest that neither activin-A or TGF-β1 changed NK cell programs induced during MCMV infection, nor did they impact on viral replication during acute infection. Thus, unlike for tumor immunotherapy, blockade of activin may not be relevant in the context of viral pathogenesis.

Validation of activin signaling in human NK cells

To further validate whether activin-A signaling was conserved between human and mouse NK cells, we examined key signal transduction pathways and markers of ILC1 cells and NK cells. Human cord blood–derived NK cells were purified and activated in medium containing donor-matched serum and IL-15, and a neutralizing antibody against either mouse or human TGF-β1/2/3 was used for 5 days to remove any TGF-β present in the serum. The cells were then exposed to rIL-15, rActivin-A, rTGF-β1, or combinations of these cytokines for different times. Assessment of the phosphorylation of signaling molecules revealed efficient phosphorylation of SMAD2/3 by either rActivin-A or rTGF-β1 irrespective of whether IL-15 was

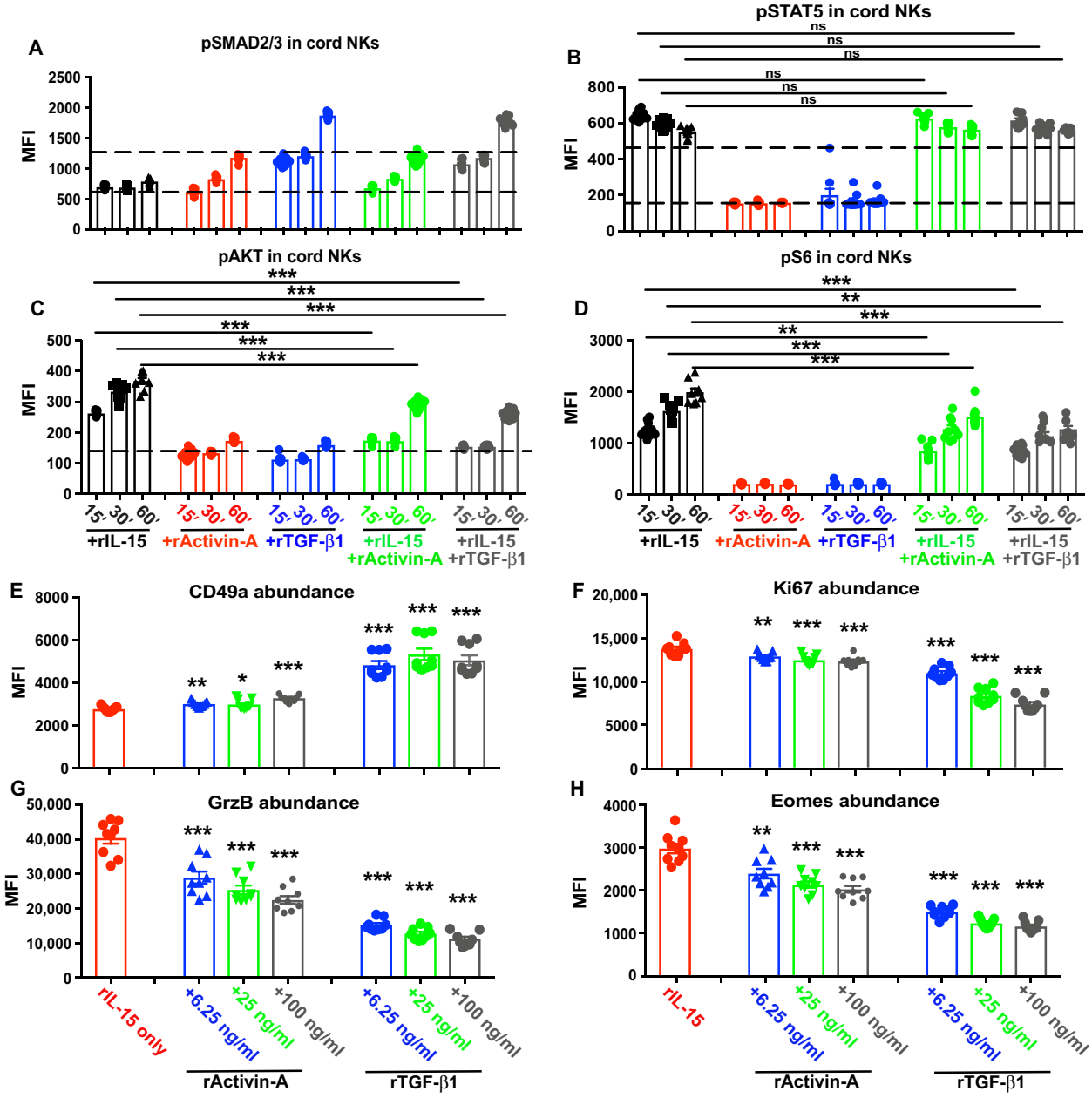

Fig. 6. Conserved features of activin signaling in human NK cells. (**A** to **H**) Human NK cells were isolated from fresh cord blood (three different donors) and primed in rIL-15 for 48 hours. The cells were then washed, starved for 4 hours in animal component–free medium at 37°C, and stimulated in medium containing rIL-15 (10 ng/ml) with or without the indicated concentrations of rActivin-A or rTGF-β1 for 1 hour. The relative abundances of pSMAD2/3 (A), pSTAT5 (B), pAKT (C), and pS6 (D) were determined by flow cytometry analysis and reported as MFI. (E to H) A portion of the same cord blood NK samples was cultured separately for 7 days in the presence of rIL-15 (50 ng/ml) with or without the indicated concentrations of rActivin-A or rTGF-β1. The cells were then surface-stained with anti-CD49a antibody (E) and intracellularly stained with anti-Ki67 (F), anti-GrzB (G), and anti-Eomes (H) antibodies, and their relative MFIs were analyzed by flow cytometry. Data are means ± SEM. Each dot on the graphs represents one independent technical replicate (with three technical replicates for each of the three donors). The unpaired *t* test was used for comparative statistical analysis. **P* < 0.05, ***P* < 0.01, and ****P* < 0.001.

present (Fig. 6A and fig. S8A). Consistent with our previous report (*13*), we observed that IL-15–induced phosphorylation of signal transducer and activator of transcription 5 (STAT5) was independent of SMAD2/3 phosphorylation (in response to either activin-A or TGF-β1) (Fig. 6B and fig. S8B). However, both activin-A and TGF-β1 suppressed the IL-15–induced phosphorylation of AKT and S6K (Fig. 6, C and D, and fig. S8, C and D), consistent with our earlier findings (Fig. 1, F and G) and our previous work on mouse NK cell metabolism (*13*).

Last, we also examined whether activin-A signaling induced the increased abundance of ILC1 markers on human NK cells, similarly to what we observed with mouse NK cells (Fig. 2). We cultured human cord blood–derived NK cells for 7 days with IL-15 in the presence of either rActivin-A or rTGF-β1. Consistent with our findings from

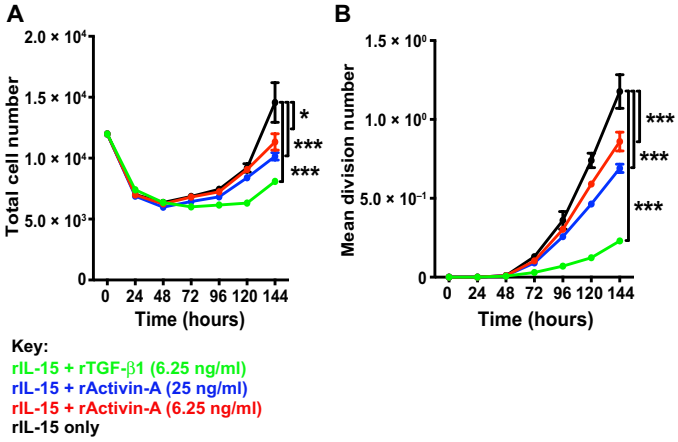

Fig. 7. Activin signaling impairs human NK cell proliferation. (**A** and **B**) Freshly isolated human cord blood–derived NK cells were labeled with a division-tracking dye and cultured in the presence of rIL-15 (50 ng/ml) and in the presence or absence of the indicated concentrations of rTGF-β1 or rActivin-A. For each condition, the total number of live cells was enumerated at 24-hour intervals (A), and the population average division number was calculated (B). Results are from one donor and are representative of three independent biological replicates. Data are means ± SD of three technical replicates. Two-way ANOVA tests were used for comparative statistical analysis. *$P < 0.05$ and ***$P < 0.001$.

experiments with mouse NK cells, we found that the cell surface abundance of CD49a was increased in a concentration-dependent manner by both rActivin-A and rTGF-β1 (Fig. 6E and fig. S8E), whereas there was a corresponding reduction in the amounts of GrzB and Ki67 (Fig. 6, F and G, and fig. S8, F and G). We also found that rActivin-A was sufficient to reduce the abundance of Eomes in human NK cells (Fig. 6H and fig. S8H). Last, similar to our findings from experiments with mouse NK cells (Fig. 1, D and E), we found that both rActivin-A and rTGF-β1 reduced the expansion of human NK cells by suppressing their proliferation rate (reduced mean division number) (Fig. 7, A and B). These findings indicate that the regulation of NK cell biology by activin-A signaling is likely conserved between humans and mice.

DISCUSSION

Immune checkpoint inhibitors have revolutionized cancer therapy by reinvigorating cytotoxic lymphocytes to kill malignant cells. NK cells have an innate ability to detect cellular transformation and are key to cancer immunosurveillance, particularly in the prevention of metastasis (*1*). An understanding of the tumor microenvironment and how tumor cells evade detection by NK cell is now emerging and has stimulated great interest in the therapeutic targeting of such pathways (*54*). We previously revealed an immune evasion mechanism in which tumors exploit the TGF-β signaling pathway to differentiate cNK cells (CD49a^{neg}) into ILC1-like subsets (CD49a^{+}) and, in doing so, reduce their intrinsic antitumor functions (*14*). An earlier study described a similar differentiation process in salivary gland NK cells (*39*). Both of these studies used the conditional deletion of the gene encoding TGF-βRII in NK cells (NKp46$^{cre/+}$*Tgfbr2*$^{fl/fl}$) as a negative control for TGF-β signaling. However, despite the fact that NKp46$^{cre/+}$*Tgfbr2*$^{fl/fl}$ NK cells are unresponsive to rTGF-β1 in vitro, both of these studies revealed the presence of a minor ILC1-like NKp46^{+}CD49a^{+} cell population in vivo in NKp46$^{cre/+}$*Tgfbr2*$^{fl/fl}$ mice. Together, these data suggest that factors other than TGF-β1 might also mediate NK cell reprogramming and tumor immune evasion.

Our work on TGF-β–dependent immune evasion mechanism by the differentiation of effector cNK cells (Eomes^{+}, CD49b^{+}, CD49a^{neg}, TRAIL^{neg}) into ILC1-like cells (Eomes^{neg}, CD49b^{neg}, CD49a^{+}, TRAIL^{+}) or intermediate ILC1 cells (Eomes^{+}, CD49b^{+}, CD49a^{+}, TRAIL^{+}) has been observed in experimental metastasis and orthotopic melanoma models, as well as for fibrosarcomas, which suggests that TGF-β can suppress both systemic and tumor-resident NK cell responses (*14*). Given our data demonstrating that activin-A acts in a similar manner to TGF-β in inducing an ILC1-like phenotype in NK cells, this finding may help to explain the presence of residual ILC1-like cells that are observed in the tumors of NKp46$^{cre/+}$*Tgfbr2*$^{fl/fl}$ mice. Our in vitro data demonstrate that activin-A induces several changes to murine and human NK cells that are reminiscent of those induced by TGF-β. These include suppression of cellular metabolism and proliferation and an increase in the abundance of ILC1-related markers. Furthermore, these changes occurred with TGF-βRII–deficient NK cells, thus ruling out any role for activin-A synergizing with TGF-β found in serum-containing culture medium. The effect of TGF-β at the concentrations (~60 pg/ml) found in culture medium (fig. S2) is noteworthy because TGF-βRII–deficient NK cells consistently appear hyperactive compared to WT NK cells when expanded in IL-15 in vitro. For example, TGF-βRII–deficient NK cells displayed substantially increased basal and maximal metabolism and produced statistically significantly more IFN-γ compared to their WT counterparts. Whereas activin-A suppressed the metabolism of TGF-βRII–deficient NK cells, it only impaired glycolysis and oxidative phosphorylation to a similar extent to that in WT NK cells cultured in the absence of activin-A, which highlights the enhanced metabolic state of TGF-βRII–deficient NK cells.

The concentration-dependent effect of activin-A on WT NK cells was exemplified in experiments examining SMAD2/3 phosphorylation, Ki67 and GrzB abundances, and impaired killing of B16F10 melanoma cells. However, NK cell metabolism and ILC1-related gene expression appeared to be maximally altered at the lowest concentrations of activin-A, highlighting the differential sensitivity of certain NK-suppressive pathways to activin-A signaling. Despite this, endogenous amounts of activin-A appeared to be sufficient to suppress NK cell activity because the therapeutic administration of FST reduced lung metastases in a NK cell–dependent melanoma model. Together, our results reveal a previously unappreciated capacity for activin-A to regulate NK cell differentiation, thereby ultimately facilitating the ability of tumors to evade NK cell–mediated immune surveillance in a TGF-β–independent manner. Our findings suggest that combinatorial therapies targeting activin signaling may result in greater prevention of cNK-ILC1–like cell differentiation in the tumor microenvironment (and the associated suppression of cellular metabolism and effector function) and subsequently enhance innate antitumor immune control.

MATERIALS AND METHODS

Mice

TGF-βRII–deficient NK cells were isolated from NKp46$^{cre/wt}$*TgfbR2*$^{fl/fl}$ mice, which were generated by crossing NKp46-iCre mice (*55*) with *TgfbR2* LoxP mice (*56*) as previously described (*13*, *14*). WT NK cells were isolated from the corresponding littermate controls (NKp46$^{wt/wt}$*TgfbR2*$^{fl/fl}$). All mice were on a C57BL/6J background

and were bred and maintained at the Walter and Eliza Hall Institute of Medical Research (WEHI). For MCMV infections, BALB/C mice were acquired from the Animal Research Centre (Perth) and housed in the Bioresources Department of the Harry Perkins. All experiments were performed using cells from an age- and sex-matched cohort of mice (age range, 8 to 12 weeks). Cohort sizes are described in each figure legend to achieve statistical significance. No biological replicate was excluded on the basis of pre-established criteria. All experiments were approved by the WEHI and Harry Perkins Institute of Animal Ethics Committees.

Reagents

Reagents or antibodies targeting the following human (h) or murine (m) epitopes were purchased from BioLegend: 7-aminoactinomycin D (7-AAD), mCD3 (145-2C11), mCD19 (6D5), mCD49b (DX5 and HMα2), mCD62L (MEL-14), mDNAM-1 (10E5), mF4/80 (BM8), mLy6G (1A8), mNK1.1 (PK136), mNKp46 (29A1.4), streptavidin-FITC (fluorescein isothiocyanate), and mTCR-β (H57-597). Reagents or antibodies targeting the following epitopes were purchased from eBioscience: mCD49b (DX5), hEomes (WD1928), mEomes (Dan11mag), mGranzyme B (NGZB), hGranzyme B (GB11), mTCR-β (H57–597), and mTRAIL (N2B2). Reagents or antibodies targeting the following epitopes were purchased from BD Biosciences: Akt(pS476) (M89-61), fixable viability stain, mNK1.1 (PK136), Ki67 (B56), SMAD2(pS465/S467)/SMAD3(pS423/pS425) (I72-670), and STAT5(pY694) (47/Stat5(pY694)). Antibody targeting pS6(pS235/S236) (#2211) was purchased from Cell Signaling Technology. Antibodies targeting mCD45.2 (30F11), mCD49a (REA493), hCD49a (TS2/7), mCD69 (H1.2F3), and hNKp46 (9E2) were purchased from Miltenyi Biotec. The MACSXpress Human NK Cell Isolation Kit (Miltenyi Biotec) was used for the negative selection of cord blood NK cells. To detect intracellular Eomes, GrzB, and Ki67, surface-stained cells were fixed and permeabilized with the Intracellular Fixation and Permeabilization Buffer Set and stained with antibodies in 1× Permeabilization Buffer (eBioscience). Cell numbers were calculated with BD Liquid Counting Beads (BD Biosciences).

NK cell isolation and culture conditions

Mice were sacrificed, and spleens were harvested and prepared for flow cytometry as previously described (*49*). Spleen homogenates were incubated in Fc blocking buffer (2.4G2 antibody) on ice for 15 min and then pre-enriched by lineage (Lin: CD3, CD19, CD49a, F4-80, Ly6G, TCRβ) biotin-antibody cocktail staining, which was followed by incubation with MagniSort Streptavidin Bead Negative Selection (eBioscience). The remaining fraction of cells was stained with streptavidin-FITC, and NK cells (7-AAD$^-$Lin$^-$CD45$^+$NK1.1$^+$NKp46$^+$CD49b$^+$) from transgenic or WT mice were then sorted with a BD FACSAria III cell sorter (BD Biosciences) to achieve a final cell purity of 99 to 100%. Human cord blood NK cells were isolated by negative selection with a final cell purity of 95 to 99% using the MACSXpress Human NK Cell Isolation Kit (Miltenyi Biotec). After sorting or negative selection, mouse or human NK cells were stained with CellTrace Violet (Invitrogen) and plated at a density of 25,000 cells per well in V bottom 96-well plates (Greiner Bio-One) containing RPMI 1640 supplemented with 10% FCS, 1% sodium pyruvate (Gibco), 1% GlutaMAX (Gibco), 10 mM Hepes, 0.1% 2-mercaptoethanol (Gibco), and 1% penicillin/streptomycin in the presence or absence of human rIL-15 (Miltenyi Biotec), human/mouse rActivin-A (R&D Systems), mouse rTGF-β1 (eBioscience), or human rTGF-β1 (PeproTech) at the concentrations and for the times indicated in the figure legends. Culture conditions were maintained at 37°C and 5% CO_2. Intracellular staining of phosphorylated signaling proteins was performed using antibodies against pAkt, pSMAD2/3, pS6, and pSTAT5 after endpoint fixation and permeabilization with Lyse/Fix and Perm III buffers (BD Biosciences). Data were acquired with an LSR Fortessa flow cytometer (BD Biosciences). Flow cytometric analysis was performed with FlowJo software (TreeStar). For proliferation and viability assays, fresh human and murine NK cells were incubated with 5 μM CellTrace Violet (Thermo Fisher Scientific) according to the manufacturer's instructions, and 8×10^3 labeled cells were seeded into 96-well round bottom plates in complete medium containing cytokines at the concentrations and for the times indicated in the figure legends. Routine time points were assessed on a BD FACSVerse cytometer (BD Biosciences), and survival and division numbers were determined using the precursor cohort-based method (*57*, *58*), as previously described for NK cell kinetics (*7*).

In vitro cytokine secretion assays

FACSAria-sorted NK cells from the spleens (Lin^{neg}, 7AAD^{neg}, CD49a^{neg}, NKp46$^+$, NK1.1$^+$, CD49b$^+$) of mice of the genotypes indicated in the figure legends were expanded for up to 10 days in complete RPMI 1640 containing 10% fetal bovine serum (FBS), anti–TGF-β1/2/3 blocking antibody (1 μg/ml; clone 1D11.16.8, Bio X Cell), β-mercaptoethanol, GlutaMAX, and sodium pyruvate (Gibco). For cytokine secretion assays, cells were stimulated with rTGF-β1, rActivin-A, or rIL-15 at the concentrations indicated in the figure legends in animal-free/TGF-β1–free TexMACS medium (Miltenyi Biotec) containing β-mercaptoethanol, GlutaMAX, and sodium pyruvate for 48 hours. For the detection of cytokines in the culture medium of cells in vitro, IFN-γ was measured by enzyme-linked immunosorbent assay (ELISA) with the respective human or murine IFN-γ DuoSet Kit (R&D Systems) according to the manufacturer's instructions, whereas all other cytokines were detected with Cytometric Bead Array (CBA) technology (BD Biosciences) according to the manufacturer's instructions.

Target:effector cell cocultures

Sorted and expanded NK cells (as described earlier) were used to perform standard 4-hour cytotoxicity assays using calcein-AM (acetoxymethyl) B16F10 melanoma cells labeled with calcein-AM (BD Biosciences), as previously described (*6*). Briefly, NK cells from mice of the genotypes indicated in the figure legends were cultured overnight (for 16 hours) in the presence of rTGF-β1 or rActivin-A at the indicated concentrations and in the presence of rIL-15 (50 ng/ml). The NK cells were then seeded at the given ratios with calcein-AM–labeled target cells in complete NK cell medium (phenol red–free RPMI 1640 containing 10% FBS, β-mercaptoethanol, GlutaMAX, and sodium pyruvate). After 4 hours of coculture, supernatants were transferred to opaque 96-well plates (Costar), and fluorescence emission was measured with an EnVision microplate reader (PerkinElmer). Cytotoxicity data were expressed as the percentage lysis relative to the spontaneous (target cells alone) and maximum release (treated cells; 1% Triton X-100, Sigma-Aldrich). In some experiments, melanoma cells were cultured on round glass coverslips and cocultured overnight in 24-well plates with purified NK cells in the indicated culture conditions.

NK cell preparation for proteomics

NK cells were sorted from the spleens of RII^{FL} or WT mice and expanded for 7 days in rIL-15 (50 ng/ml) in RPMI 1640 medium containing 10% FCS supplemented with neutralizing TGF-β1/2/3 antibody (1D11.16.8). Cells were then washed three times with ice-cold phosphate-buffered saline (PBS) and starved in serum-free medium for 4 hours, and then 5×10^6 cells per replicate/culture condition were cultured in medium containing rIL-15 (10 ng/ml) with rTGF-β1 (6.25 ng/ml) or rActivin-A (25 ng/ml) for 24 hours. Cells (3×10^6) from mice of each genotype and stimulation condition ($n = 4$ per group) were then washed three times with ice-cold PBS before undergoing dry cell pellet storage at −80°C. Cells were lysed in preheated (95°C) 5% SDS/10 mM tris/10 mM tris (2-carboxyethyl) phosphine/5.5 mM 2-chloroacetamide and heated at 95°C for 10 min. Neat trifluoracetic acid (Sigma) was added to hydrolyze the DNA, resulting in a final concentration of 1%. Lysates were quenched with 4 M tris (pH 10), resulting in a final concentration of ~140 mM tris (pH 7). NK cell protein lysates (~60 μg) were prepared for mass spectrometry (MS) analysis as described by Dagley *et al.* (*59*). For all experiments with magnetic beads, a 1:1 combination mix of the two types of commercially available carboxylate beads (Sera-Mag SpeedBeads, #45152105050250 and #65152105050250, GE Healthcare) was used. Beads were prepared freshly each time by rinsing with water three times before use and storage at 4°C at a stock concentration of 20 μg/μl. Carboxylate beads (4 μl) were added to all samples together with acetonitrile [ACN; final concentration, 70% (v/v)] and incubated at room temperature for 18 min. Samples were then placed on a magnetic rack, supernatants were discarded, and the beads were washed twice with 70% ethanol and once with neat ACN (180-μl washes). ACN was completely evaporated from the tubes using a CentriVap (Labconco) before the addition of 40 μl of digestion buffer (10% trifluoroethanol/100 mM NH_4HCO_3) containing Lys-C (Wako, 129-02541) and Trypsin Gold (Promega, V5280) each at a 1:50 enzyme/substrate ratio. Enzymatic digestions proceeded for 1 hour at 37°C using the ThermoMixer C (Eppendorf) shaking at 400 rpm. After the digest, samples were placed on a magnetic rack, the supernatants containing peptides were collected, and an additional elution (50 μl) was performed with 2% dimethyl sulfoxide (Sigma) before sonication in a water bath for 1 min. The eluates were pooled together and transferred to the top of pre-equilibrated C18 StageTips (4× plugs of 3 M Empore resin, #2215) for sample cleanup as previously described (*60*). The eluates were lyophilized to dryness using a CentriVap (Labconco) before being reconstituted in 30 μl of 0.1% formic acid/2% ACN ready for MS analysis.

MS analysis

Peptides (2 μl) were separated by reversed-phase chromatography on a 1.6-μm C18 fused silica column (inner diameter 75 μm, outer diameter 360 μm × 25 cm length) packed into an emitter tip (IonOpticks) using a nano-flow high-performance liquid chromatography (HPLC) (M-class, Waters). The HPLC was coupled to an Impact II UHR-QqTOF mass spectrometer (Bruker) using a CaptiveSpray source and nanoBooster at 0.20 bar using ACN. Peptides were loaded directly onto the column at a constant flow rate of 400 nl/min with buffer A (99.9% Milli-Q water and 0.1% formic acid) and eluted with a 90-min linear gradient from 2 to 34% buffer B (99.9% ACN and 0.1% formic acid). Mass spectra were acquired in a data-dependent manner including an automatic switch between MS and MS/MS scans using a 1.5-s duty cycle and 4-Hz MS1 spectra rate followed by MS/MS scans at 8 to 20 Hz dependent on precursor intensity for the remainder of the cycle. MS spectra were acquired between a mass range of 200 and 2000 m/z (mass-to-charge ratio). Peptide fragmentation was performed using collision-induced dissociation. For data analysis, raw files consisting of high-resolution MS/MS spectra were processed with MaxQuant (version 1.5.8.3) for feature detection and protein identification using the Andromeda search engine (*61*). Extracted peak lists were searched against the *Mus musculus* database (UniProt, October 2016), as well as a separate reverse decoy database to empirically assess the false discovery rate (FDR) using strict trypsin specificity, allowing up to two missed cleavages. The minimum required peptide length was set to seven amino acids. In the main search, precursor mass tolerance was 0.006 Da and fragment mass tolerance was 40 parts per million (ppm). The search included variable modifications of oxidation (methionine), N-terminal acetylation, the addition of pyroglutamate (at the N termini of glutamate and glutamine), and a fixed modification of carbamidomethyl (cysteine). The "match between runs" option in MaxQuant was used to transfer identifications made between runs on the basis of matching precursors with high mass accuracy (*62*). Peptide spectrum matches and protein identifications were filtered using a target-decoy approach at an FDR of 1%.

Seahorse assays

For seahorse assays, NK cells were stimulated overnight (for 20 hours) in medium containing rIL-15 (100 ng/ml) together with the concentrations of rActivin-A or rTGF-β1 indicated in the figure legends, washed three times in PBS, and incubated for 3 hours in Seahorse XF Media unbuffered glucose-free Dulbecco's modified Eagle's medium (Seahorse Bioscience) containing rIL-15 (5 ng/ml). Stimulated cells were then transferred to 0.5% gelatin-coated seahorse plates (Seahorse Bioscience), suspended in 160 μl of Seahorse XF Media, and then stimulated with 40 μl of the same medium containing a final concentration (per well) of 25 mM glucose, 1 μM oligomycin, 1.5 M FCCP, 1 mM sodium pyruvate, 1 μM antimycin A, and 0.1 μM rotenone. OCRs and ECARs were measured every 7 min using a Seahorse XF^e96 analyzer (Seahorse Bioscience).

FST-specificity bioassay

The activin-responsive luciferase reporter A3-Lux or the BMP-responsive luciferase reporter BRE-Lux was used to measure the bioactivity of FST. Human embryonic kidney (HEK) 293 T cells were plated on poly-lysine–coated 24-well plates at a density of 150,000 cells per well. Approximately 24 hours later, the cells were transfected with A3-Lux (25 ng) or BRE-Lux (100 ng) using Lipofectamine 2000 transfection reagent (Invitrogen). Sixteen hours after transfection, the cells were treated with 0.2 nM activin-A, BMP2, or BMP7 together with increasing concentrations of FST (0 to 2 nM). After 16 hours, the cells were harvested in solubilization buffer [1% Triton X-100, 25 mM glycine (pH 7.8), 15 mM $MgSO_4$, 4 mM EGTA, and 1 mM dithiothreitol], and luciferase reporter activity was then measured according to standard protocols.

In vivo assays

In vivo models were performed as previously described for intravenous inoculation of 2×10^5 or 4×10^5 B16F10 cells (*49*) or systemic MCMV infection with 5×10^3 plaque-forming units (PFU) of MCMV-K181 intraperitoneally (*53*). Treatments were performed blinded, and the code was revealed with witnesses at the end of the experiments and data analysis: Clinical-grade activin-A inhibitor,

FST (provided by Paranta Biosciences Ltd., Melbourne, Australia), was intraperitoneally administrated with daily doses of 10 μg per mouse as indicated in the figure legends; neutralizing anti–TGF-β1/2/3 antibody clone 1D11.16.8 or the corresponding control immunoglobulin G1 (IgG1) (Bio X Cell) was administrated every 3 days with intraperitoneally administered doses of 500 μg per mouse as indicated in the figure legends. At the endpoint of the MCMV infections (day 6 after intraperitoneal viral inoculation), organs were processed for antibody staining and flow cytometric analysis as indicated in the figure legends, and MCMV viral titers in organs were determined by plaque assay using M210B4 cells as previously described (*49*, *53*).

Statistical analysis

Statistical analysis was performed with GraphPad Prism software v6. The statistical tests used were the unpaired *t* test, paired *t* tests for seahorse assays, and the two-way analysis of variance (ANOVA) test for cytotoxicity and proliferation experiments. Error bars represent SEM or SD, as indicated in the figure legends. Levels of statistical significance were expressed as *P* values: $^{*}P < 0.05$, $^{**}P < 0.01$, and $^{***}P < 0.001$. For the label-free quantitative proteomics pipeline, statistically significant changes in protein abundance between the RII^{FL} and control groups were identified using a custom-designed, in-house pipeline, as previously described (*6*), where quantitation was performed at the peptide level. Probability values were corrected for multiple testing using the Benjamini-Hochberg method (*63*). Cutoff lines with the function $y = -\log_{10}(0.05) + c/(x - x_0)$ (*64*) were introduced to identify statistically significantly enriched proteins. *c* was set to 0.2, whereas x_0 was set to 1, representing proteins with a twofold ($\log_2$ protein ratios of ≥1 or more) or fourfold ($\log_2$ protein ratio of 2) change in protein abundance, respectively.

SUPPLEMENTARY MATERIALS

stke.sciencemag.org/cgi/content/full/12/596/eaat7527/DC1

Fig. S1. Analysis of the expression of alternative activin receptors.
Fig. S2. Analysis of basal amounts of TGF-β1 in culture medium.
Fig. S3. Analysis of total NK cell cohort numbers after treatment with activin-A or TGF-β.
Fig. S4. Analysis of the effects of rActivin-A and rTGF-β1 on NK cell activation.
Fig. S5. Analysis of the inhibitory effect of FST.
Fig. S6. Analysis of NK cell surface markers.
Fig. S7. Analysis of the effects of FST in vivo.
Fig. S8. Conserved features of activin-A signaling in human NK cells.
Table S1. Summary of the $\log_2$ fold change and *P* values associated with the label-free quantitative proteomics experiments.

REFERENCES AND NOTES

1. Y. Krasnova, E. M. Putz, M. J. Smyth, F. Souza-Fonseca-Guimaraes, Bench to bedside: NK cells and control of metastasis. *Clin. Immunol.* **177**, 50–59 (2017).
2. F. Souza-Fonseca-Guimaraes, NK cell-based immunotherapies: Awakening the innate anti-cancer response. *Discov. Med.* **21**, 197–203 (2016).
3. P. A. Beavis, U. Divisekera, C. Paget, M. T. Chow, L. B. John, C. Devaud, K. Dwyer, J. Stagg, M. J. Smyth, P. K. Darcy, Blockade of A2A receptors potently suppresses the metastasis of $CD73^{+}$ tumors. *Proc. Natl. Acad. Sci. U.S.A.* **110**, 14711–14716 (2013).
4. P. A. Beavis, N. Milenkovski, J. Stagg, M. J. Smyth, P. K. Darcy, A2A blockade enhances anti-metastatic immune responses. *Oncoimmunology* **2**, e26705 (2013).
5. X. Liu, N. Shin, H. K. Koblish, G. Yang, Q. Wang, K. Wang, L. Leffet, M. J. Hansbury, B. Thomas, M. Rupar, P. Waeltz, K. J. Bowman, P. Polam, R. B. Sparks, E. W. Yue, Y. Li, R. Wynn, J. S. Fridman, T. C. Burn, A. P. Combs, R. C. Newton, P. A. Scherle, Selective inhibition of IDO1 effectively regulates mediators of antitumor immunity. *Blood* **115**, 3520–3530 (2010).
6. R. B. Delconte, T. B. Kolesnik, L. F. Dagley, J. Rautela, W. Shi, E. M. Putz, K. Stannard, J.-G. Zhang, C. Teh, M. Firth, T. Ushiki, C. E. Andoniou, M. A. Degli-Esposti, P. P. Sharp, C. E. Sanvitale, G. Infusini, N. P. D. Liau, E. M. Linossi, C. J. Burns, S. Carotta, D. H. D. Gray, C. Seillet, D. S. Hutchinson, G. T. Belz, A. I. Webb, W. S. Alexander, S. S. Li, A. N. Bullock, J. J. Babon, M. J. Smyth, S. E. Nicholson, N. D. Huntington, CIS is a potent checkpoint in NK cell-mediated tumor immunity. *Nat. Immunol.* **17**, 816–824 (2016).
7. C. Viant, S. Guia, R. J. Hennessy, J. Rautela, K. Pham, C. Bernat, W. Goh, Y. Jiao, R. Delconte, M. Roger, V. Simon, F. Souza-Fonseca-Guimaraes, S. Grabow, G. T. Belz, B. T. Kile, A. Strasser, D. Gray, P. D. Hodgkin, B. Beutler, E. Vivier, S. Ugolini, N. D. Huntington, Cell cycle progression dictates the requirement for BCL2 in natural killer cell survival. *J. Exp. Med.* **214**, 491–510 (2017).
8. P. Sathe, R. B. Delconte, F. Souza-Fonseca-Guimaraes, C. Seillet, M. Chopin, C. J. Vandenberg, L. C. Rankin, L. A. Mielke, I. Vikstrom, T. B. Kolesnik, S. E. Nicholson, E. Vivier, M. J. Smyth, S. L. Nutt, S. P. Glaser, A. Strasser, G. T. Belz, S. Carotta, N. D. Huntington, Innate immunodeficiency following genetic ablation of *Mcl1* in natural killer cells. *Nat. Commun.* **5**, 4539 (2014).
9. N. D. Huntington, H. Puthalakath, P. Gunn, E. Naik, E. M. Michalak, M. J. Smyth, H. Tabarias, M. A. Degli-Esposti, G. Dewson, S. N. Willis, N. Motoyama, D. C. S. Huang, S. L. Nutt, D. M. Tarlinton, A. Strasser, Interleukin 15-mediated survival of natural killer cells is determined by interactions among Bim, Noxa and Mcl-1. *Nat. Immunol.* **8**, 856–863 (2007).
10. D. H. Raulet, S. Gasser, B. G. Gowen, W. Deng, H. Jung, Regulation of ligands for the NKG2D activating receptor. *Annu. Rev. Immunol.* **31**, 413–441 (2013).
11. D. M. Benson Jr., M. A. Caligiuri, Killer immunoglobulin-like receptors and tumor immunity. *Cancer Immunol. Res.* **2**, 99–104 (2014).
12. M. M. Rahim, A. P. Makrigiannis, Ly49 receptors: Evolution, genetic diversity, and impact on immunity. *Immunol. Rev.* **267**, 137–147 (2015).
13. S. Viel, A. Marcais, F. S.-F. Guimaraes, R. Loftus, J. Rabilloud, M. Grau, S. Degouve, S. Djebali, A. Sanlaville, E. Charrier, J. Bienvenu, J. C. Marie, C. Caux, J. Marvel, L. Town, N. D. Huntington, L. Bartholin, D. Finlay, M. J. Smyth, T. Walzer, TGF-β inhibits the activation and functions of NK cells by repressing the mTOR pathway. *Sci. Signal.* **9**, ra19 (2016).
14. Y. Gao, F. Souza-Fonseca-Guimaraes, T. Bald, S. S. Ng, A. Young, S. F. Ngiow, J. Rautela, J. Straube, N. Waddell, S. J. Blake, J. Yan, L. Bartholin, J. S. Lee, E. Vivier, K. Takeda, M. Messaoudene, L. Zitvogel, M. W. L. Teng, G. T. Belz, C. R. Engwerda, N. D. Huntington, K. Nakamura, M. Hölzel, M. J. Smyth, Tumor immunoevasion by the conversion of effector NK cells into type 1 innate lymphoid cells. *Nat. Immunol.* **18**, 1004–1015 (2017).
15. L. Kubiczkova, L. Sedlarikova, R. Hajek, S. Sevcikova, TGF-β - an excellent servant but a bad master. *J. Transl. Med.* **10**, 183 (2012).
16. F. Ghiringhelli, C. Ménard, M. Terme, C. Flament, J. Taieb, N. Chaput, P. E. Puig, S. Novault, B. Escudier, E. Vivier, A. Lecesne, C. Robert, J.-Y. Blay, J. Bernard, S. Caillat-Zucman, A. Freitas, T. Tursz, O. Wagner-Ballon, C. Capron, W. Vainchencker, F. Martin, L. Zitvogel, $CD4^{+}CD25^{+}$ regulatory T cells inhibit natural killer cell functions in a transforming growth factor-β–dependent manner. *J. Exp. Med.* **202**, 1075–1085 (2005).
17. F. Souza-Fonseca-Guimaraes, M. J. Smyth, Myeloid TGF-β responsiveness promotes metastases. *Cancer Discov.* **3**, 846–848 (2013).
18. G. Bellone, M. Aste-Amezaga, G. Trinchieri, U. Rodeck, Regulation of NK cell functions by TGF-β 1. *J. Immunol.* **155**, 1066–1073 (1995).
19. C. L. Arteaga, S. D. Hurd, A. R. Winnier, M. D. Johnson, B. M. Fendly, J. T. Forbes, Anti-transforming growth factor (TGF)-beta antibodies inhibit breast cancer cell tumorigenicity and increase mouse spleen natural killer cell activity. Implications for a possible role of tumor cell/host TGF-beta interactions in human breast cancer progression. *J. Clin. Invest.* **92**, 2569–2576 (1993).
20. Y. Shi, J. Massague, Mechanisms of TGF-β signaling from cell membrane to the nucleus. *Cell* **113**, 685–700 (2003).
21. S. Lin, K. K. H. Svoboda, J. Q. Feng, X. Jiang, The biological function of type I receptors of bone morphogenetic protein in bone. *Bone Res.* **4**, 16005 (2016).
22. H. A. Loomans, C. D. Andl, Activin receptor-like kinases: A diverse family playing an important role in cancer. *Am. J. Cancer Res.* **6**, 2431–2447 (2016).
23. S. Pasteuning-Vuhman, J. W. Boertje-van der Meulen, M. van Putten, M. Overzier, P. Ten Dijke, S. M. Kielbasa, W. Arindrarto, R. Wolterbeek, K. V. Lezhnina, I. V. Ozerov, A. M. Aliper, W. M. Hoogaars, A. Aartsma-Rus, C. J. Loomans, New function of the myostatin/activin type I receptor (ALK4) as a mediator of muscle atrophy and muscle regeneration. *FASEB J.* **31**, 238–255 (2017).
24. N. C. Robson, D. J. Phillips, T. McAlpine, A. Shin, S. Svobodova, T. Toy, V. Pillay, N. Kirkpatrick, D. Zanker, K. Wilson, I. Helling, H. Wei, W. Chen, J. Cebon, E. Maraskovsky, Activin-A: A novel dendritic cell-derived cytokine that potently attenuates CD40 ligand-specific cytokine and chemokine production. *Blood* **111**, 2733–2743 (2008).
25. K. L. Jones, D. M. de Kretser, S. Patella, D. J. Phillips, Activin A and follistatin in systemic inflammation. *Mol. Cell. Endocrinol.* **225**, 119–125 (2004).
26. S. Huber, F. R. Stahl, J. Schrader, S. Lüth, K. Presser, A. Carambia, R. A. Flavell, S. Werner, M. Blessing, J. Herkel, C. Schramm, Activin a promotes the TGF-β-induced conversion of $CD4^{+}CD25$- T cells into $Foxp3^{+}$ induced regulatory T cells. *J. Immunol.* **182**, 4633–4640 (2009).
27. M. Semitekolou, T. Alissafi, M. Aggelakopoulou, E. Kourepini, H. H. Kariyawasam, A. B. Kay, D. S. Robinson, C. M. Lloyd, V. Panoutsakopoulou, G. Xanthou, Activin-A induces regulatory T cells that suppress T helper cell immune responses and protect from allergic airway disease. *J. Exp. Med.* **206**, 1769–1785 (2009).

28. M. Bashir, S. Damineni, G. Mukherjee, P. Kondaiah, Activin-A signaling promotes epithelial–mesenchymal transition, invasion, and metastatic growth of breast cancer. *NPJ Breast Cancer* **1**, 15007 (2015).
29. M. Basu, R. Bhattacharya, U. Ray, S. Mukhopadhyay, U. Chatterjee, S. S. Roy, Invasion of ovarian cancer cells is induced byPITX2-mediated activation of TGF-β and Activin-A. *Mol. Cancer* **14**, 162 (2015).
30. J. Cursons, K.-J. Leuchowius, M. Waltham, E. Tomaskovic-Crook, M. Foroutan, C. P. Bracken, A. Redfern, E. J. Crampin, I. Street, M. J. Davis, E. W. Thompson, Stimulus-dependent differences in signalling regulate epithelial-mesenchymal plasticity and change the effects of drugs in breast cancer cell lines. *Cell Commun. Signal.* **13**, 26 (2015).
31. M. A. Hoda, A. Rozsas, E. Lang, T. Klikovits, Z. Lohinai, S. Torok, J. Berta, M. Bendek, W. Berger, B. Hegedus, W. Klepetko, F. Renyi-Vamos, M. Grusch, B. Dome, V. Laszlo, High circulating activin A level is associated with tumor progression and predicts poor prognosis in lung adenocarcinoma. *Oncotarget* **7**, 13388–13399 (2016).
32. M. Antsiferova, A. Piwko-Czuchra, M. Cangkrama, M. Wietecha, D. Sahin, K. Birkner, V. C. Amann, M. Levesque, D. Hohl, R. Dummer, S. Werner, Activin promotes skin carcinogenesis by attraction and reprogramming of macrophages. *EMBO Mol. Med.* **9**, 27–45 (2017).
33. K. L. Walton, Y. Makanji, C. A. Harrison, New insights into the mechanisms of activin action and inhibition. *Mol. Cell. Endocrinol.* **359**, 2–12 (2012).
34. P. Donovan, O. A. Dubey, S. Kallioinen, K. W. Rogers, K. Muehlethaler, P. Müller, D. Rimoldi, D. B. Constam, Paracrine activin-A signaling promotes melanoma growth and metastasis through immune evasion. *J. Invest. Dermatol.* **137**, 2578–2587 (2017).
35. D. D. Seachrist, S. T. Sizemore, E. Johnson, F. W. Abdul-Karim, K. L. Weber Bonk, R. A. Keri, Follistatin is a metastasis suppressor in a mouse model of HER2-positive breast cancer. *Breast Cancer Res.* **19**, 66 (2017).
36. J. Nishida, K. Miyazono, S. Ehata, Decreased TGFBR3/betaglycan expression enhances the metastatic abilities of renal cell carcinoma cells through TGF-β-dependent and -independent mechanisms. *Oncogene* **37**, 2197–2212 (2018).
37. N. C. Robson, H. Wei, T. McAlpine, N. Kirkpatrick, J. Cebon, E. Maraskovsky, Activin-A attenuates several human natural killer cell functions. *Blood* **113**, 3218–3225 (2009).
38. H. Spits, D. Artis, M. Colonna, A. Diefenbach, J. P. Di Santo, G. Eberl, S. Koyasu, R. M. Locksley, A. N. J. McKenzie, R. E. Mebius, F. Powrie, E. Vivier, Innate lymphoid cells—A proposal for uniform nomenclature. *Nat. Rev. Immunol.* **13**, 145–149 (2013).
39. V. S. Cortez, L. Cervantes-Barragan, M. L. Robinette, J. K. Bando, Y. Wang, T. L. Geiger, S. Gilfillan, A. Fuchs, E. Vivier, J. C. Sun, M. Cella, M. Colonna, Transforming growth factor-β signaling guides the differentiation of innate lymphoid cells in salivary glands. *Immunity* **44**, 1127–1139 (2016).
40. S. Lotinun, R. S. Pearsall, W. C. Horne, R. Baron, Activin receptor signaling: A potential therapeutic target for osteoporosis. *Curr. Mol. Pharmacol.* **5**, 195–204 (2012).
41. R. B. Delconte, W. Shi, P. Sathe, T. Ushiki, C. Seillet, M. Minnich, T. B. Kolesnik, L. C. Rankin, L. A. Mielke, J.-G. Zhang, M. Busslinger, M. J. Smyth, D. S. Hutchinson, S. L. Nutt, S. E. Nicholson, W. S. Alexander, L. M. Corcoran, E. Vivier, G. T. Belz, S. Carotta, N. D. Huntington, The helix-loop-helix protein ID2 governs NK cell fate by tuning their sensitivity to interleukin-15. *Immunity* **44**, 103–115 (2016).
42. M. L. Holmes, N. D. Huntington, R. P. Thong, J. Brady, Y. Hayakawa, C. E. Andoniou, P. Fleming, W. Shi, G. K. Smyth, M. A. Degli-Esposti, G. T. Belz, A. Kallies, S. Carotta, M. J. Smyth, S. L. Nutt, Peripheral natural killer cell maturation depends on the transcription factor Aiolos. *EMBO J.* **33**, 2721–2734 (2014).
43. C. Seillet, N. D. Huntington, P. Gangatirkar, E. Axelsson, M. Minnich, H. J. Brady, M. Busslinger, M. J. Smyth, G. T. Belz, S. Carotta, Differential requirement for Nfil3 during NK cell development. *J. Immunol.* **192**, 2667–2676 (2014).
44. A. Herpin, C. Lelong, P. Favrel, Transforming growth factor-β-related proteins: An ancestral and widespread superfamily of cytokines in metazoans. *Dev. Comp. Immunol.* **28**, 461–485 (2004).
45. I. Bank, M. Book, R. Ware, Functional role of VLA-1 (CD49A) in adhesion, cation-dependent spreading, and activation of cultured human T lymphocytes. *Cell. Immunol.* **156**, 424–437 (1994).
46. D. K. Sojka, B. Plougastel-Douglas, L. Yang, M. A. Pak-Wittel, M. N. Artyomov, Y. Ivanova, C. Zhong, J. M. Chase, P. B. Rothman, J. Yu, J. K. Riley, J. Zhu, Z. Tian, W. M. Yokoyama, Tissue-resident natural killer (NK) cells are cell lineages distinct from thymic and conventional splenic NK cells. *eLife* **3**, e01659 (2014).
47. C. Fionda, M. P. Abruzzese, A. Zingoni, F. Cecere, E. Vulpis, G. Peruzzi, A. Soriani, R. Molfetta, R. Paolini, M. R. Ricciardi, M. T. Petrucci, A. Santoni, M. Cippitelli, The IMiDs targets IKZF-1/3 and IRF4 as novel negative regulators of NK cell-activating ligands expression in multiple myeloma. *Oncotarget* **6**, 23609–23630 (2015).
48. T. A. Fehniger, S. F. Cai, X. Cao, A. J. Bredemeyer, R. M. Presti, A. R. French, T. J. Ley, Acquisition of murine NK cell cytotoxicity requires the translation of a pre-existing pool of granzyme B and perforin mRNAs. *Immunity* **26**, 798–811 (2007).
49. F. Souza-Fonseca-Guimaraes, A. Young, D. Mittal, L. Martinet, C. Bruedigam, K. Takeda, C. E. Andoniou, M. A. Degli-Esposti, G. R. Hill, M. J. Smyth, NK cells require IL-28R for optimal in vivo activity. *Proc. Natl. Acad. Sci. U.S.A.* **112**, E2376–E2384 (2015).
50. K. H. Gartlan, K. A. Markey, A. Varelias, M. D. Bunting, M. Koyama, R. D. Kuns, N. C. Raffelt, S. D. Olver, K. E. Lineburg, M. Cheong, B. E. Teal, M. Lor, I. Comerford, M. W. L. Teng, M. J. Smyth, J. McCluskey, J. Rossjohn, B. Stockinger, G. M. Boyle, S. W. Lane, A. D. Clouston, S. R. McColl, K. P. A. MacDonald, G. R. Hill, Tc17 cells are a proinflammatory, plastic lineage of pathogenic $CD8^+$ T cells that induce GVHD without antileukemic effects. *Blood* **126**, 1609–1620 (2015).
51. X. Wang, W. Ma, S. Han, Z. Meng, L. Zhao, Y. Yin, Y. Wang, J. Li, TGF-β participates choroid neovascularization through Smad2/3-VEGF/TNF-α signaling in mice with Laser-induced wet age-related macular degeneration. *Sci. Rep.* **7**, 9672 (2017).
52. J. M. Yingling, W. T. McMillen, L. Yan, H. Huang, J. S. Sawyer, J. Graff, D. K. Clawson, K. S. Britt, B. D. Anderson, D. W. Beight, D. Desaiah, M. M. Lahn, K. A. Benhadji, M. J. Lallena, R. B. Holmgaard, X. Xu, F. Zhang, J. R. Manro, P. W. Iversen, C. V. Iyer, R. A. Brekken, M. D. Kalos, K. E. Driscoll, Preclinical assessment of galunisertib (LY2157299 monohydrate), a first-in-class transforming growth factor-β receptor type I inhibitor. *Oncotarget* **9**, 6659–6677 (2017).
53. I. S. Schuster, M. E. Wikstrom, G. Brizard, J. D. Coudert, M. J. Estcourt, M. Manzur, L. A. O'Reilly, M. J. Smyth, J. A. Trapani, G. R. Hill, C. E. Andoniou, M. A. Degli-Esposti, $TRAIL^+$ NK cells control $CD4^+$ T cell responses during chronic viral infection to limit autoimmunity. *Immunity* **41**, 646–656 (2014).
54. F. Souza-Fonseca-Guimaraes, J. Cursons, N. D. Huntington, The emergence of natural killer cells as a major target in cancer immunotherapy. *Trends Immunol.* **40**, 142–158 (2019).
55. E. Narni-Mancinelli, J. Chaix, A. Fenis, Y. M. Kerdiles, N. Yessaad, A. Reynders, C. Gregoire, H. Luche, S. Ugolini, E. Tomasello, T. Walzer, E. Vivier, Fate mapping analysis of lymphoid cells expressing the NKp46 cell surface receptor. *Proc. Natl. Acad. Sci. U.S.A.* **108**, 18324–18329 (2011).
56. P. Levéen, J. Larsson, M. Ehinger, C. M. Cilio, M. Sundler, L. J. Sjöstrand, R. Holmdahl, S. Karlsson, Induced disruption of the transforming growth factor beta type II receptor gene in mice causes a lethal inflammatory disorder that is transplantable. *Blood* **100**, 560–568 (2002).
57. E. D. Hawkins, M. Hommel, M. L. Turner, F. L. Battye, J. F. Markham, P. D. Hodgkin, Measuring lymphocyte proliferation, survival and differentiation using CFSE time-series data. *Nat. Protoc.* **2**, 2057–2067 (2007).
58. J. M. Marchingo, A. Kan, R. M. Sutherland, K. R. Duffy, C. J. Wellard, G. T. Belz, A. M. Lew, M. R. Dowling, S. Heinzel, P. D. Hodgkin, T cell signaling. Antigen affinity, costimulation, and cytokine inputs sum linearly to amplify T cell expansion. *Science* **346**, 1123–1127 (2014).
59. L. F. Dagley, G. Infusini, R. H. Larsen, J. J. Sandow, A. I. Webb, Universal Solid-Phase Protein Preparation (USP3) for Bottom-up and Top-down Proteomics. *J. Proteome Res.* **18**, 2915–2924 (2019).
60. J. Rappsilber, M. Mann, Y. Ishihama, Protocol for micro-purification, enrichment, pre-fractionation and storage of peptides for proteomics using StageTips. *Nat. Protoc.* **2**, 1896–1906 (2007).
61. J. Cox, N. Neuhauser, A. Michalski, R. A. Scheltema, J. V. Olsen, M. Mann, Andromeda: A peptide search engine integrated into the MaxQuant environment. *J. Proteome Res.* **10**, 1794–1805 (2011).
62. J. Cox, M. Mann, MaxQuant enables high peptide identification rates, individualized p.p.b.-range mass accuracies and proteome-wide protein quantification. *Nat. Biotechnol.* **26**, 1367–1372 (2008).
63. D. H. Glueck, J. Mandel, A. Karimpour-Fard, L. Hunter, K. E. Muller, Exact calculations of average power for the Benjamini-Hochberg procedure. *Int. J. Biostat.* **4**, Article 11 (2008).
64. E. C. Keilhauer, M. Y. Hein, M. Mann, Accurate protein complex retrieval by affinity enrichment mass spectrometry (AE-MS) rather than affinity purification mass spectrometry (AP-MS). *Mol. Cell. Proteomics* **14**, 120–135 (2015).

Acknowledgments: We thank all the members of the Huntington laboratory for discussion, comments, and advice on this project and A. Campbell, E. Surgenor, E. Loza, T. Camilleri, and T. Kratina for mouse breeding, maintenance, genotyping, and technical support. We thank S. Karlsson for providing the *TgfbR2* floxed mice and B.K. (Paranta Biosciences Ltd.) for clinical-grade FST for the in vivo assays. **Funding:** This work was supported by project grants from the National Health and Medical Research Council (NHMRC) of Australia (grants 1124784, 1066770, 1057852, and 1124907 to N.D.H.; grant 1140406 to F.S.-F.-G.; and NHMRC Program grant 1071822 to M.A.D.-E.). F.S.-F.-G. was supported by an NHMRC Early Career Fellowship (1088703), a National Breast Cancer Foundation (NBCF) Fellowship (PF-15-008), grants 1120725 and 1158085 awarded through the Priority-driven Collaborative Cancer Research Scheme, and the Cure Cancer Australia with the assistance of Cancer Australia. N.D.H. is an NHMRC CDF2 Fellow (1124788) and a recipient of a Melanoma Research Grant from the

Harry J. Lloyd Charitable Trust, a Melanoma Research Alliance Young Investigator Award, a Tour De Cure research grant, an equipment grant from The Ian Potter Foundation, and a CLIP grant from Cancer Research Institute. M.A.D.-E. holds a NHMRC Principal Research Fellowship (1119298). This study was made possible through Victorian State Government Operational Infrastructure Support and the Australian Government NHMRC Independent Research Institute Infrastructure Support scheme. **Author contributions:** A.I.W., C.C.d.O., C.H., D.S.H., J.R., I.S.S., J.C., L.F.D., M.J.D., M.A.D.-E., R.B.D., R.H., S.H.-Z., and F.S.-F.-G. designed, performed research, and analyzed data. E.V. and B.K. provided key reagents and scientific input into interpretation of the results. N.D.H. and F.S.-F.-G. supervised work and wrote the paper. **Competing interests:** N.D.H. and J.R. are cofounders and shareholders in oNKo-Innate. N.D.H., J.R., and F.S.-F.-G. have a funded research collaborative agreement with Paranta Bioscience Ltd. E.V. is a cofounder and shareholder in Innate Pharma. The other authors declare that they have no competing interests. **Data and materials availability:** The MS proteomics data were deposited in the ProteomeXchange Consortium through the PRIDE partner repository with the dataset identifier PXD011672. All data needed to evaluate the conclusions in the paper are present in the paper or the Supplementary Materials.

Submitted 30 March 2018
Resubmitted 13 November 2018
Accepted 13 August 2019
Published 27 August 2019
10.1126/scisignal.aat7527

Citation: J. Rautela, L. F. Dagley, C. C. de Oliveira, I. S. Schuster, S. Hediyeh-Zadeh, R. B. Delconte, J. Cursons, R. Hennessy, D. S. Hutchinson, C. Harrison, B. Kita, E. Vivier, A. I. Webb, M. A. Degli-Esposti, M. J. Davis, N. D. Huntington, F. Souza-Fonseca-Guimaraes, Therapeutic blockade of activin-A improves NK cell function and antitumor immunity. *Sci. Signal.* **12**, eaat7527 (2019).

Therapeutic blockade of activin-A improves NK cell function and antitumor immunity

Jai Rautela, Laura F. Dagley, Carolina C. de Oliveira, Iona S. Schuster, Soroor Hediyeh-Zadeh, Rebecca B. Delconte, Joseph Cursons, Robert Hennessy, Dana S. Hutchinson, Craig Harrison, Badia Kita, Eric Vivier, Andrew I. Webb, Mariapia A. Degli-Esposti, Melissa J. Davis, Nicholas D. Huntington and Fernando Souza-Fonseca-Guimaraes

Sci. Signal. **12** (596), eaat7527.
DOI: 10.1126/scisignal.aat7527

Enhancing NK cells

Natural killer (NK) cells are innate immune cells with a critical role in antitumor immunity. In the tumor microenvironment, the cytokine transforming growth factor–β (TGF-β) acts through its receptor to promote the differentiation of NK cells into a less suppressive cell type, thus inhibiting antitumor immunity. Rautela *et al.* showed that activin-A, another member of the TGF- β family, had similar effects on both mouse and human NK cells, although in a TGF- β receptor –independent manner. Inhibition of activin-A reduced orthotopic melanoma growth in mice, suggesting that targeting this pathway could therapeutically enhance NK cell function and antitumor immunity.